

Original Research

Development of a guar gum film with lysine clonixinate for periodontal treatments

Cassandra Marilú Robles-Kanafany¹, María Luisa Del Prado-Audelo^{1,2,*}, Maykel González-Torres³, David M. Giraldo-Gomez^{4,5}, Isaac H. Caballero-Florán¹, Manuel González-Del Carmen⁶, Javad Sharifi-Rad^{7,8}, Gabriela Figueroa-González⁹, Octavio D. Reyes-Hernández¹⁰, Hernán Cortés¹¹, Gerardo Leyva-Gómez^{1*}

¹Departamento de Farmacia, Facultad de Química, Universidad Nacional Autónoma de México, Ciudad de México 04510, Mexico

²Escuela de Ingeniería y Ciencias, Departamento de Bioingeniería, Tecnológico de Monterrey Campus Ciudad de México, Ciudad de México 14380, Mexico

³CONACyT-Laboratorio de Biotecnología, Instituto Nacional de Rehabilitación Luis Guillermo Ibarra Ibarra, Ciudad de México 14389, Mexico

⁴Departamento de Biología Celular y Tisular, Facultad de Medicina, Universidad Nacional Autónoma de México, Ciudad de México, 04510, Mexico

⁵Unidad de Microscopía, Facultad de Medicina, Universidad Nacional Autónoma de México, Ciudad de México, 04510, Mexico

⁶Facultad de Medicina, Universidad Veracruzana, Mendoza 94740, Veracruz, Mexico

⁷Phytochemistry Research Center, Shahid Beheshti University of Medical Sciences, Tehran, Iran

⁸Facultad de Medicina, Universidad del Azuay, Cuenca, Ecuador

⁹Laboratorio de Farmacogenética, UMIEZ, Facultad de Estudios Superiores Zaragoza, Universidad Nacional Autónoma de México, Ciudad de México 09230, Mexico

¹⁰Laboratorio de Biología Molecular del Cáncer, UMIEZ, Facultad de Estudios Superiores Zaragoza, Universidad Nacional Autónoma de México, Ciudad de México 09230, Mexico

¹¹Laboratorio de Medicina Genómica, Departamento de Genómica, Instituto Nacional de Rehabilitación-Luis Guillermo Ibarra Ibarra, Ciudad de México 14389, Mexico

*Correspondence to: luisa.delpradoa@gmail.com; leyva@quimica.unam.mx

Received August 7, 2020; Accepted November 10, 2020; Published January 31, 2021

Doi: <http://dx.doi.org/10.14715/cmb/2021.67.1.13>

Copyright: © 2021 by the C.M.B. Association. All rights reserved.

Abstract: Periodontal pain is a public health problem derived from different conditions, including periodontal diseases, prosthetic complications, and even extractions performed by dentist. There are various treatments to control acute dental pain, being the administration of analgesics, such as Lysine Clonixinate (LC), a common practice. Unfortunately, higher and repeated dosages are usually required. The purpose of this work was to develop a prolonged release pharmaceutical form as an alternative treatment for dental pain. Hence, we conceived a film based on guar gum and loaded different concentrations of LC. We evaluated the film's appearance, brittleness, strength, and flexibility, and then chose one formulation for adequate characteristics. Subsequently, we assessed the morphology, thermal behavior, and swelling properties of the films (LC-free and -loaded). Finally, we performed the release studies of LC from the films *in vitro* using a simulated saliva medium and employed several mathematical models to evaluate the release kinetics. Guar gum is a natural polymer obtained from the endosperm of *Cyamopsis tetragonolobus* that presents properties such as biosafety, biocompatibility, and biodegradability. Thus, it represents a potential excipient for use in pharmaceutical formulations. Moreover, our results revealed that the LC-loaded film presented a high adherence, suitable swelling behavior, high LC content, and a prolonged drug release. Therefore, the LC-loaded film may be considered a potential option to be applied as an alternative to treat dental pain.

Key words: Natural polymers; Guar gum; Polymeric film; Periodontal diseases; Lysine clonixinate; Solving-casting.

Introduction

Periodontal pain is a condition generated by diseases such as periodontal disease (gingivitis, periodontitis), pericoronitis, and dental surgical procedures (1). According to the FDI World Dental Federation, periodontal diseases affect 50% of the world population; thus, it is a public health problem. This disease affects the gums, causing inflammation and damaging the bones and supporting tissue (2). The usual treatment for this type of condition includes analgesics, anesthetics, and antibiotics (1). An analgesic commonly used in periodontal disease is Lysine Clonixinate (LC) due to its high safety and efficacy. However, its frequency of administration varies from 3-4 dosages a day with a dose of 125-250

mg (3). Thus, new dosage forms for its administration are needed.

In this context, films are an excellent option since they are flexible, thin, easy to handle; moreover, they possess high drug loading capacity and longer residence time (4). Different natural and synthetic materials can be applied for the development of these films (5,6). Guar gum (GG) is a polymer of natural origin used in cosmetics, food, and pharmaceutical formulations. It is mainly used as a stabilizing thickener and provides a controlled release to solid pharmaceutical forms (7). This polymer is obtained from the endosperm of the *Cyamopsis tetragonolobus* seeds and is composed of mannose and galactose (8). GG presents good biodegradability and low toxicity, making it an excellent candidate for drug

delivery developments (9). Furthermore, it is rich in hydroxyl groups, responsible for the viscosity and thickness of the polymer solutions. Likewise, this property permits the formation of non-covalent bonds with biological tissues such as epithelial and mucous, giving rise to adhesion, another expected feature in materials with potential application in drug delivery systems (4,10,11). On the other hand, Polyvinylpyrrolidone (PVP) is a polymer used to formulate drug delivery systems due to its ease of film formation and stabilizer capacity (owing to the specific conformation of the chains). Moreover, it is a biocompatible and non-toxic polymer used in the pharmaceutical area to develop numerous administration systems (12). In this work, we developed an LC-loaded polymeric film based on GG and PVP to reduce the frequency of administration, intending to administer it on a single occasion. We characterized the film by several techniques such as scanning electron microscopy (SEM), thermogravimetric analysis (TGA), swelling capacity, among others. Interestingly, the film presented a swelling that gave rise to a prolonged-release profile reaching 20 h. According to our promising results, we propose this film as an adjunct treatment without neglecting antibiotics, scaling curettage, and root planing.

Materials and Methods

For the preparation of the films, LC was obtained from Maver. GG and Propylene Glycol were purchased from Cosmopolita Drugstore (Mexico). PVP (Kollidon 30) was acquired from BASF (USA).

For the preparation of the Simulated Saliva Medium (SSM), citric acid was obtained from Barsa. Dibasic Sodium Phosphate and Monobasic Potassium Phosphate were acquired from J.T.Baker (USA). Calcium Carbonate was purchased from Paris Drugstore (Mexico). Calcium Chloride, Potassium Chloride, and Sodium Chloride were acquired from Cosmopolita Drugstore (Mexico).

Preparation of the film

The film (described as M) was obtained by the solvent-casting method, based on the solvent evaporation. The first step consisted of elaborating a gel of the GG and PVP K30 polymers with different percentages of propylene glycol (Table 1). Propylene glycol was dissolved in an aqueous medium maintaining constant stirring at 40 °C. Subsequently, GG and PVP K30 were incorporated. Finally, the mixture was deposited in Teflon molds of 12 cm in diameter; each mold was placed in an oven at 35 ± 5 °C to eliminate the water. Based on physical characteristics, only one formulation was chosen to load LC (abbreviated as M-LC) (Table 2). Subsequent analyzes were only carried out with formulation 10E (M-LC) because it contained a higher dose of LC.

Physical evaluation of films

All polymeric films were visually evaluated, taking into account their appearance, brittleness, strength, flexibility. For the appearance, the opacity or transparency of the films was considered. Moreover, the fragility and resistance were evaluated by manipulating the films.

Determination of dimensions

A batch of 5 films was fabricated for each formulation with LC; 10A, 10B, 10C, 10D, and 10E (M-LC), all under the same conditions. After drying, the diameter and thickness of the films were measured (Digital Caliper, HER-411, Steren).

Morphological analysis by SEM

The microstructure of the selected films (M, M-LC) was analyzed by SEM (Carl ZEISS Crossbeam 550 FIB SEM Instrument, Bengaluru, Karnataka) to determine the surface roughness and corroborate thickness. The samples were coated with a thin layer of gold by plasma-assisted deposition using the JEOL Fine Coat ION JFC-1100 equipment.

Index of swelling

In order to evaluate the swelling capacity, 1 cm² of the M-LC formulation previously weighed was placed in a test tube (also previously weighed). The samples were placed in 500 µL of SSM (Table 3), and the analysis of swelling was carried out at times: 15, 30, 45, 60, 75, 90, 105, 120, 135, 150, 165, and 180 min. Each sample was analyzed in triplicate. Subsequently, the SSM tubes were discarded, and each one was weighed. Afterward, the swelling percentage was calculated using the following formula:

$$\text{Index of swelling (\%)} = \frac{w_2 - w_1}{w_1} * 100$$

Where w_2 is the weight of the wet films and w_1 is the weight of the dry films.

Thermal analysis

Thermal properties were determined using a thermogravimetric analyzer (Hi-res TGA 2950, New Castle, USA). The samples were analyzed from room temperature to 500 °C with a heating flow of 10 °C/min under a nitrogen atmosphere.

Quantification of dose uniformity

A dose uniformity test was carried out to guarantee that the film has the required drug content. Samples were placed in 500 mL of SSM, maintaining constant agitation for 24 h to simulate the mouth conditions. Subsequently, a sample was taken, and its absorbance was measured at $\lambda = 320.0$ nm (DLAB SP-UV 1000, Beijing, China).

Dissolution profile

Samples of 1 cm² of M and M-LC were placed in beakers with 80 mL of SSM solution; each film was fixed to the inner wall of the beaker in a water bath with shaking at 37 ± 5 °C (13). Three mL was taken at different times (15, 30, 45, 120, 150, 180, 360, 600, and 720 min). The LC released in the SMM was quantified by UV-visible spectrophotometry at 320 nm (DLAB SP-UV 1000, Beijing, China).

Drug release models

The data analysis of the release profile was carried out in the DDSolver software to know the drug exit mechanism from the film.

Results

Preparation of the films and physical evaluation

First, we used different percentages of excipients for the film's development; the results are shown in Table 1. According to our results, the least opaque, more resistant, flexible, and with the best appearance formulation was the batch 10. Therefore, we chose this batch to be employed as the administration form.

After the film selection, we fabricated several films with different concentrations of LC; the results are exhibited in Table 2.

Determination of film dimensions

We measured the dimensions of the films 10A to 10E to analyze the variations on thickness due to the LC incorporation (see Table 3). The thickness of the film's formulations did not vary, while the diameter of the films was affected concerning the LC content from 77 to 100 mm. Based on this behavior, we selected the 10E film as the best candidate due to the higher concentration of LC. This film was named as M-LC.

Morphological analysis by SEM

We assessed the morphology of the films M and

M-LC by SEM. As can be observed, the M-LC (Fig. 1a and 1c) presented pores in the middle and cracks. The morphology of M also presented pores in the transversal cut, but the surface did not present cracks (Fig. 1b and 1d).

Swelling index

We determined the swelling index in SSM (Table 4). Figure 2 depicts the behavior of M and M-LC analyzed for three hours. In the case of M, we observed a decrease in swelling after 135 min, while M-LC had a continuous increase.

Thermogravimetric analysis

The thermograms of the excipients used and the films (M and M-LC) are presented in Figure 3. As shown, the GG thermogram (line A) only showed a weight loss between 250-320 °C. The thermogram corresponding to the PVP (line C) revealed two significant weight losses, the first one between 380-454 °C, and the second one in the range of 550-630 °C. For propylene glycol (line B), a significant weight loss started at 190 °C and completely decomposed at nearly 225 °C. For LC (line D), the initial temperature of the mass loss was approximately 180 °C, ending at 280 °C. On the other hand, M (Line

Table 1. Formulation of films with GG, PVP K30, and propylene glycol.

Batch	Guar Gum %(w/w)	PVP K30 %(w/w)	Propylene glycol %(w/w)	Physical characteristics
1	1.0	0.5	0.5	Homogeneous, opaque, fragile
2	1.0	0.5	1.0	Homogeneous, opaque, fragile
3	1.0	0.5	1.5	Homogeneous, opaque, fragile
4	1.0	0.5	2.0	Homogeneous, opaque, fragile
5	1.0	0.5	2.5	Homogeneous, opaque, fragile
6	1.0	0.5	3.0	Homogeneous, opaque, resistant (++), supple (+)
7	1.0	0.5	3.5	Homogeneous, opaque, resistant (++), supple (+)
8	1.0	0.5	4.0	Homogeneous, opaque, resistant (++), supple (++)
9	1.0	0.5	4.5	Homogeneous, opaque, resistant (++), supple (++)
10	1.0	0.5	5.0	Homogeneous, opaque, resistant (++), supple (++)

The characteristics were evaluated according to a qualitative scale where the levels correspond to Low (+), Medium (++), and High (+++).

Table 2. Formulation of M-LC at different concentrations of LC.

Batch	Guar Gum %(w/w)	PVP K30 %(w/w)	Propylene glycol %(w/w)	LC (mg)	Physical characteristics
10A	1.0	0.5	5.0	200.0	Homogeneous, translucent, resistant (++), supple (+)
10B	1.0	0.5	5.0	400.0	Homogeneous, translucent, resistant (+++), supple (+)
10C	1.0	0.5	5.0	600.0	Homogeneous, translucent, resistant (+++), supple (+++)
10D	1.0	0.5	5.0	800.0	Homogeneous, supple (++) , adherent (++)
10E	1.0	0.5	5.0	1000.0	Homogeneous, supple (++) , adherent (++)

The characteristics were evaluated according to a qualitative scale where the levels correspond to Low (+), Medium (++), and High (+++).

Table 3. Films dimensions with different formulations with LC.

Films	10A	10B	10C	10D	10E
Dose (mg)	200	400	600	800	1000
Average thickness (mm)	0.56	0.56	0.56	0.5	0.44
Thickness deviation	0.15	0.19	0.11	0.12	0.09
Average diameter (mm)	77.62	82.04	92.48	100.64	89.62
Diameter deviation	3.70	3.98	3.59	1.31	1.96

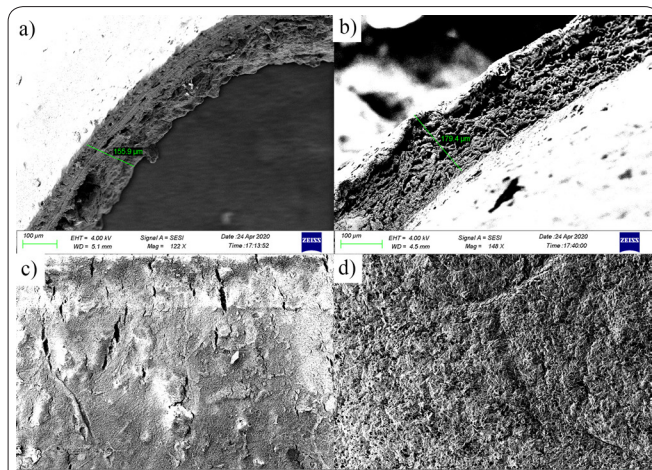


Figure 1. Morphological analysis by SEM. a) Image of M-LC, view of the films after carrying out a cross-section with a thickness of 155.9 μm (magnification 122 X, the measuring bar is equivalent to 100 μm), b) Image of M, view of the films after carrying out a cross-section with a thickness of 179.4 μm (magnification 148 X, the measuring bar is equivalent to 100 μm), c) Image of M-LC surface (magnification 100 X, the measuring bar is equivalent to 100 μm), and d) Image of M surface (magnification 55 X, the measuring bar is equivalent to 200 μm).

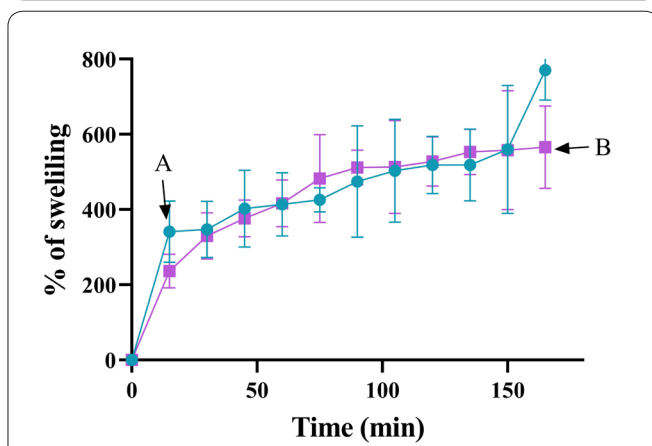


Figure 2. Percentage of swelling of the films as a function of time, corresponding to (A) M and (B) the M-LC. (mean ± SD, n = 3).

E) presented thermal events close to 170 °C, 274 °C, 368 °C, and 412 °C; meanwhile, M-LC (line F) exhibited weight losses to 106 °C, 244 °C, 282 °C, 311 °C, and 420 °C, respectively.

Quantification of dose uniformity

Table 5 indicates the doses corresponding to the M-LC samples. These amounts were between 90 to 98%, which complies with the proposed required percentage that corresponds to 85-115%.

Dissolution profile of LC

The dissolution profile of LC is shown in Fig. 4. We found that 25% of the drug was released during the first

Table 4. Composition of Simulated Saliva Medium (14).

Composition	g/L	Composition	g/L
Potassium chloride	0.720	Sodium phosphate dibasic	0.866
Calcium chloride	0.220	Potassium thiocyanate	0.060
Sodium chloride	0.600	Citric acid	0.030
Potassium phosphate monobasic	0.680		

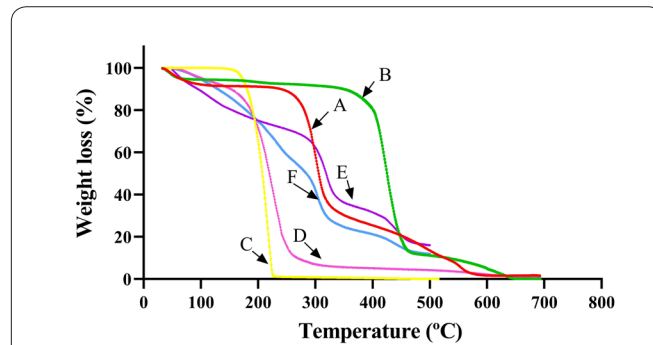


Figure 3. TGA analysis. (A) GG, (B) PVP K30, (C) Propylene glycol, (D) LC, (E) M, and (F) M-LC.

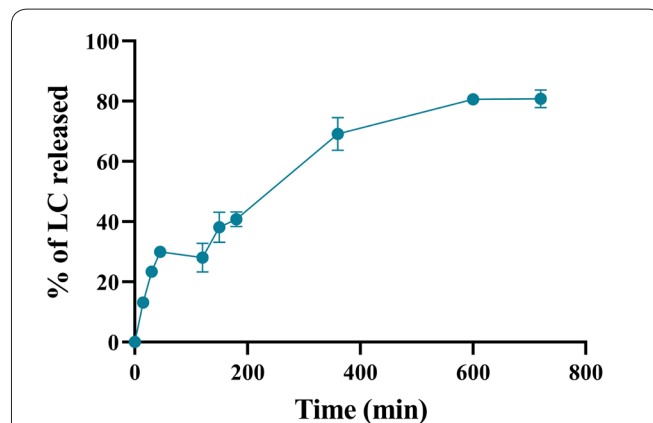


Figure 4. Percentage of LC release as a function of time corresponding to M-LC (mean ± SD, n = 3).

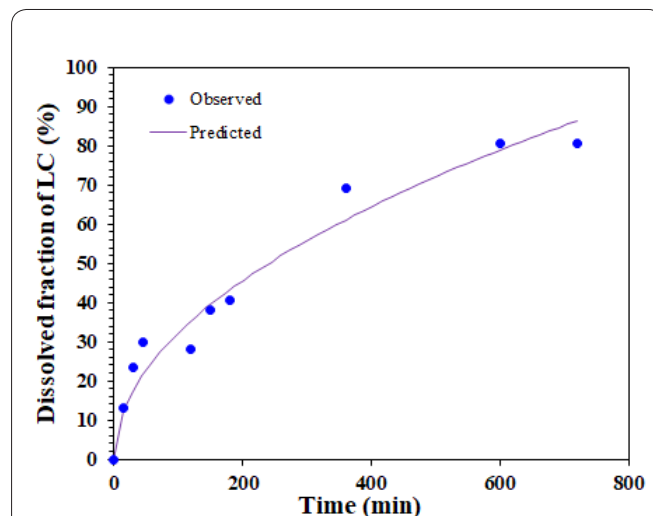


Figure 5. Adjustment of the M-LC release profile.

hour; after this time, a gradual release was observed. After 12 h of the test, about 80% of LC was released.

Drug release models

In order to predict the release behavior of LC from the films, we adjusted the drug release data by several mathematical models (Table 6). According to our re-

Table 5. Dose uniformity of LC calculated from absorbance obtained at $\lambda=320.0$ nm.

	Sample 1	Sample 2	Sample 3	Average	Deviation
Content	924.42 mg	905.67 mg	981.54 mg	937.21 mg	-----
% of LC	92.42 %	90.56 %	98.15 %	93.72 %	3.95

Table 6. Comparison between the model fit of the data obtained for the films with LC

Model	Equation	No. of parameters	R ² adjusts	AIC	MSC
Zero Order	$F = F_0 + K_0 t$	10	0.6275	80.1248	0.5778
First Order	$F = 100(1 - e^{-k_1 t})$	10	0.9040	67.1121	1.8790
Higuchi	$F = K_H t^{1/2}$	10	0.9627	57.6766	2.8226
Korsmeyer-Peppas	$F = K_{kp} t^n$	10	0.9611	58.8993	2.7003
Hixson-Crowell	$F = 100*(1 - (1 - K_{hc} t)^3)$	10	0.8626	70.7013	1.5201
Weibull	$F = 100*(1 - e^{-\frac{(t-T_i)^{\beta}}{\alpha}})$	10	0.9435	63.3068	2.2596

Where AIC (Akaike Information Criterion) and MSC (Model Selection Criterion) are parameters to adjust each model; F is the fraction of drug released at a given time; F_0 is the initial fraction of drug in solution resulting from sudden release; α is the scale parameter that defines the time scale of the process; T_i is the location parameter that represents the delay time before the start of the dissolution or release process, and in most cases, it will be close to zero; K_0 , K_1 , K_H , K_k are release rate constants; R^2 is the squared correlation coefficient.

sults, the Higuchi model was adequate to describe drug release (Figure 5).

Discussion

The correlation between the morphology of a drug delivery system and the drug release from the films is a critical aspect in evaluating new dosages forms. The M-LC film presented a more dense morphology compared with M (Fig. 1.a and Fig.1.b, respectively). This behavior is related to the presence of the LC, which triggers a compact structure. Furthermore, the surface of the M-LC presented cracks and a certain level of roughness (Fig. 1.c). Conversely, we observed a porous structure in the surface of M films (Fig. 1.d). The absence of porosity in M-LC surface is related to the high percentage of LC loaded. These observations are consistent with previous studies describing that PVP forms pore in films, and their size is according to PVP weight and concentration. In contrast, GG films presented a smooth and homogeneous surface, although with fractures (13,15). Therefore, by combining both polymers, our films had amorphous pores, which allow water diffusion through them and exploit the subsequent swelling, diffusion, and release (16).

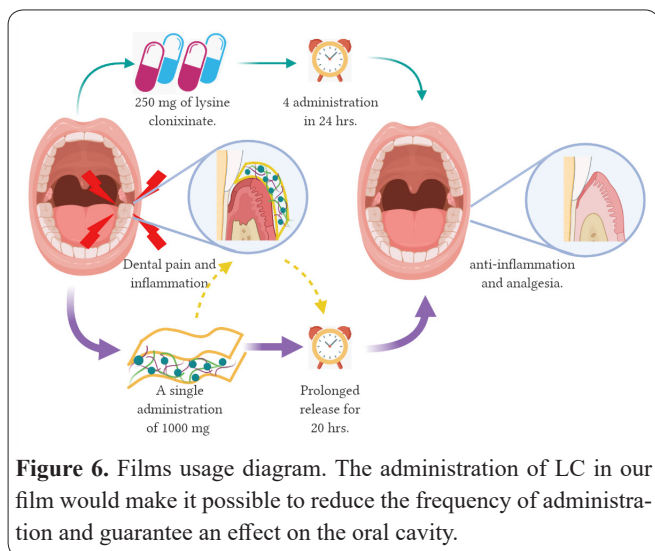
On the other hand, the wettability of the surface and the penetration of water are other crucial aspects of the film's dosage behavior. In this context, both films showed a considerable swelling percentage, presenting the maximum value between 200 and 600%. The high swelling behavior of both films could be explained by the high hydrophilicity of both principal components (GG and PVP K30) (4,17), which would facilitate the penetration of water. Likewise, the hydroxyl groups from mannose, galactose, and propylene glycol could increase molecular interactions through hydrogen bridge-type bonds (18). However, due to these conditions, it was only possible to control the films' swelling for approximately three hours because, after this time, the films gave rise to an adherent gel. Additional-

ly, since both polymers are soluble in water, the films began to solubilize after the initial three hours. This is an important parameter since the final form of the films was dense and compact, which reduces the mobility of the molecules. In this regard, when the films were in contact with the SSM, the water diffused into the system, inducing the chains relaxing, incrementing the system volume, causing swelling and the subsequently drug release from the matrix by diffusion (19).

In order to analyze the thermal properties of the excipients and the films, we carried out TGA. We observed a weight loss for GG consistent with the literature (20). Similarly, the substantial weight losses for PVP were also in agreement with previous studies. These mass losses correspond to the loss of moisture from the sample (between 380-454 °C) (21) and the decomposition of the polymer (between 550-630 °C) (22). We observed a significant loss for propylene glycol between 190-225 °C; according to Toxqui et al. (23), polyols have thermal events between 160-240°C, close to that obtained experimentally. For LC, an enormous weight difference was observed between 170-250 °C close to the drug's melting point, which is between 208-214 °C (24). Finally, the thermograms corresponding to M and M-LC films exhibited numerous thermal events that can be attributed to the interactions and cohesion forces between the excipients in their formulation.

We quantified the drug by spectrophotometry technique to evaluate the uniformity in the contents of LC in the films. According to the United States Pharmacopeia, the required percentage of drug present in an area of 1 cm² has to be 85-115% (25). Remarkably, we obtained values between 90 and 98%; thus, all the tested samples complied with the required quantity.

Moreover, we evaluated the dissolution profile in SSM to know the amount of LC released in similar conditions to the periodontal tissue. The low release rate observed in the first three hours could be related to the film's swelling and erosion in the time, in agreement with the observed result in the swelling test. After



this time, higher swelling and continuous drug release were triggered to obtain a percentage of release close to 100% after 12 h. Subsequently, we adjusted our data to different mathematical models to evaluate the possible release mechanism of LC. The Higuchi model exhibited the R^2 values closest to 0.99, the lower Akaike Information Criterion, and the higher Model Selection Criterion (26); thus, the behavior of our film followed this model. The Higuchi model assumes that drug release is based on some assumptions such as 1) the concentration of the drug at time zero must be greater than its solubility, 2) the pharmaceutical formulation must be a thin film, 3) the size of the drug particles is much less than the thickness of the film, 4) it does not swell or dissolves, and 5) the diffusion of the drug is constant (16,27). This model describes the release of water-soluble drugs from a matrix, based on a pseudo-steady-state, assuming proportionality between the amount of drug released and the square root of time (28). Therefore, our results indicate that the combination of excipients and their interaction promoted a gradual and prolonged release (19). This characteristic makes the M-LC a potential dosage strategy due to the prolonged-release performed (29).

Finally, the results obtained in the SEM images indicated a highly homogeneous structure. Hence, we conclude that the polymeric chains were compactly ordered, explaining the drug release delay. The morphology, the swelling, and the profile release confirmed the prolonged release, which would represent an advantage in long-term treatments. Furthermore, the films presented high adherence, which could be useful in terms of the collocation in the buccal zone. We present a graphical resume of the mechanism and the advantages of the M-LC as an LC administration form in Figure 6.

Tests related to the quality of M-LC film demonstrated that the film dimensions were equivalent between each of the units and their expected content. The SEM analysis revealed that the M-LC films were more uniform than the films without the drug, which explains the swelling and release profile. The mechanism of release was defined by the Higuchi model, where the diffusion is the principal phenomena.

A limited amount of formulations exist for the local treatment of dental diseases. Therefore, based on the present results, our novel film could be considered a potential option for dental conditions since it presented

a high adherence, suitable swelling behavior, high LC content, and prolonged drug release. However, toxicological evaluations and further analyses are required to support this assumption.

Acknowledgments

This research was funded by CONACYT A1-S-15759 to Gerardo Leyva-Gómez. The authors thank Karla Erieth Reyes-Morales, for her technical assistance with thermal tests, Ana Bobadilla-Valencia for her technical aid with nitrogen handling used in the experimental setting. The authors also thank Elba Carrasco Ramirez, Irma Elena López Martínez, and Ivonne Grisel Sánchez Cervantes from the Microscopy Core Facility from the School of Medicine at the UNAM for their technical assistance with microscopy assessment.

Conflicts of Interest

The authors declare no conflict of interest.

References

- Henry M, Maurin JC, Couble, Marie Lise Shibukawa Y, Tsumura M, Thivichon-Prince B, Bleicher F. Dental pain and odontoblasts: facts and hypotheses. *J Orofac Pain.* 2010;24(4):335–49.
- Severin T. Salud y enfermedades periodontales. Guía práctica para reducir la carga mundial de morbilidad para las enfermedades periodontales. 2018. p. 1–35.
- Bruschi ML, De Freitas O. Oral bioadhesive drug delivery systems. *Drug Dev Ind Pharm.* 2005;31(3):293–310.
- M. P. Prospective of guar gum and its derivatives as controlled drug delivery systems. *Int J Biol Macromol.* 2011;49(2):117–24.
- Cortes H, Caballero-Floran I, Mendoza-Muñoz N, Cordova-Villanueva E, Escutia-Guadarrama L, Figueroa-Gonzalez G, et al. Hyaluronic acid in wound dressings. *Cell Mol Biol.* 2020;66(4):192–9.
- Cortes H, Caballero-Floran IH, Mendoza-Muñoz N, Escutia-Guadarrama L, Figueroa-González G, Reyes-Hernández OD, et al. Xanthan gum in drug release. *Cell Mol Biol [Internet].* 2020 Jun 25;66(4):199–207. Available from: <https://www.cellmolbiol.org/index.php/CMB/article/view/3723>
- Mudgil D, Barak S, Khatkar BS. Guar gum: processing, properties and food applications—a review. *J Food Sci Technol.* 2011;51(3):409–18.
- Thombare N, Jha U, Mishra S, Siddiqui. Guar gum as a promising starting material for diverse applications: A review. *Int J Biol Macromol.* 2016;88:361–72.
- George A, Shah PA, Shrivastay PS. Guar gum: Versatile natural polymer for drug delivery applications. *Eur Polym J.* 2019;112:722–35.
- Koland M, Charyulu RN, Vijayanarayana K, Prabhu P. In vitro and in vivo evaluation of chitosan buccal films of ondansetron hydrochloride. *Int J Pharm Investig.* 2011;1(3):164–72.
- Bhatta R, Hossain MS, Banik S, Moghal MR, Or RM, Akter M. Swelling and mucoadhesive behavior with drug release characteristics of gastoretentive drug delivery system based on a combination of natural gum and semi-synthetic polymers. *Marmara Pharm J.* 2018;22(2):286–98.
- Franco P, De Marco I. The Use of Poly(N-vinyl pyrrolidone) in the Delivery of Drugs: A Review. *Polymers (Basel).* 2020;12(5):1114.
- Wypych TC, Andrezza IF. Development and Evaluation of a Hydrophilic Matrix as a Buccoadhesive System Containing Diclofenac Sodium. *Brazilian Arch Biol Technol.* 2011;54(5):893–900.
- Marques MRC, Loebenberg R, Almukainzi M. Simulated biological fluids with possible application in dissolution testing. *Dissolu-*

tion Technol. 2011;18(3):15–28.

15. Yeo HT, Lee ST, Han MJ. Role of a Polymer Additive in Casting Solution in Preparation of Phase Inversion Polysulfone Membranes. *J Chem Eng JAPAN*. 2000;33(1):180–4.

16. Siepmann J, Siepmann F. Mathematical modeling of drug delivery. *Int J Pharm*. 2008;364(2):328–43.

17. Awasthi R, Manchanda S, Das P, Velu V, Malipeddi H, Pabreja K, et al. In *Engineering of Biomaterials for Drug Delivery Systems*. 2018. 255–272 p.

18. Guadarrama Acevedo MC, Mendoza Flores RA, Del Prado Audelo ML, Urban Morlan Z, Giraldo Gomez DM, Magaña JJ, et al. Development and Evaluation of Alginate Membranes with Curcumin-Loaded Nanoparticles for Potential Wound-Healing Applications. *Pharmaceutics*. 2019;11(8):386.

19. Paolini MS, Fenton OS, Bhattacharya C, Andresen JL, Langer R. Polymers for extended-release administration. *Biomed Microdevices*. 2019;21(2):1–24.

20. Mudgil D, Barak S, Kratkar BS. X-ray diffraction, IR spectroscopy and thermal characterization of partially hydrolyzed guar gum. *Int J Biol Macromol*. 2012;50:1035–9.

21. Sen K, Manchanda A, Mehta T, Ma AWK, Chaudhuri B. Formulation design for inkjet-based 3D printed tablets. *Int J Pharm*. 2020;584:119430.

22. Hongbo T, Yanping L, Min S, Xiguang W. Preparation and property of crosslinking guar gum. *Polym Synth React*. 2012;44:211–6.

23. Toxqui-Terán A, Leyva-Porras C, Ruíz-Cabrera M ángel, Cruz-Alcantar P, Saavedra-Leos MZ. Thermal study of polyols for the technological application as plasticizers in food industry. *Polymers (Basel)*. 2018;10(5):1–13.

24. Royal Society Of Chemistry. Clonixin Lisine | C19H25CIN4O4 | ChemSpider. 2020.

25. Convention TUSP. U.S. USP 38-NF 33. *Pharmacopeia*. 2014. 195–197 p.

26. Zhang Y, Huo M, Zhou J, Zou A, Li W, Yao C, et al. DDSolver: An Add-In Program for Modeling and Comparison of Drug Dissolution Profiles. *AAPS J*. 2010;12(3):263–71.

27. Costa P, Sousa Lobo JM. Modeling and comparison of dissolution profiles. *Eur J Pharm Sci*. 2001;13(2):123–33.

28. Paarakh MP, Jose PANI, Setty CM, Peter G V. Release Kinetics – Concepts and Applications. *Int J Pharm Res Technol*. 2019;8(1):12–20.

29. Marcellín J, Angeles A, García A, Morales M, Rivera L, A MDC. Bioequivalence of 250 mg lysine clonixinate tablets after a single oral dose in a healthy female Mexican population under fasting conditions. *Int J Clin Pharmacol Ther*. 2010;48(5):349.